AD-A072 217 NAVY UNDERWATER SOUND LAB NEW LONDON CT F/G 17/1
BROADBAND VELOCITY CONTROL.(U)
JUN 65 D T PORTER
UNCLASSIFIED USL-TM-960-47-65 NL

| OF |
ADA
072217

END
DATE
FILMED
9-79
DDC

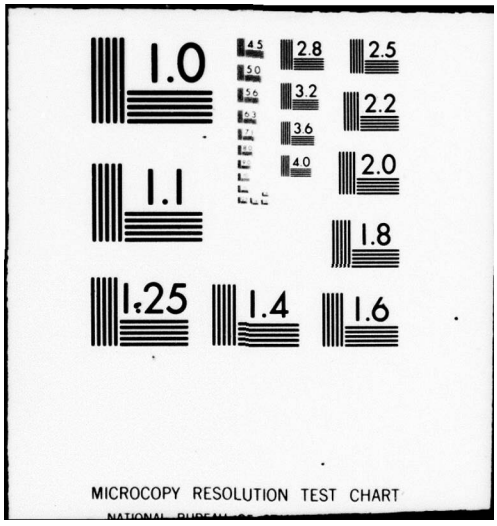
1.0
1.1
1.25
1.4
1.6
1.8
2.0
2.2
2.5
2.8
3.2
3.6
4.0
4.5
5.0
5.6
MICROCOPY RESOLUTION TEST CHART

Hudson Labs (E. Arace)

LEVEL II

COPY NO. 28

USL Tech. Memo.
1-452-00-00
S-F001 03 18-11213

COLUMBIA UNIVERSITY
HUDSON LABORATORIES
CONTRACT Nonr-266(84)

(12) 32 p'

U. S. Navy Underwater Sound Laboratory
Fort Trumbull, New London, Connecticut

(6) BROADBAND VELOCITY CONTROL.

By

(9) Technical memo,

(10) David T. Porter

USL Technical Memorandum No. 960-47-65

(11) 30 Jun 65

30 June 1965

DISTRIBUTION STATEMENT A
Approved for public release;
Distribution Unlimited

DDC
RECEIVED
AUG 6 1979
A

AD A072217

DDC FILE COPY

INTRODUCTION

Among the requirements for future sonar transmitting arrays will undoubtedly be three items: broader bands, lower frequencies, and higher power. The problem of velocity control will be concerned with all three of these requirements. (16) F00103 (17) SF001038

The requirement of broader bands complicates the problem of obtaining velocity control by electrical tuning. One can say that an array has complete velocity control if the amplitude and phase relationships between the input voltages are preserved in the transducer face velocities. At some frequencies it is possible to maintain very close velocity control by proper choice of a tuning reactor, but if a wide band of operation is required, one will have to be content with less than perfect velocity control over most of the band, unless the tuning reactor can be changed.

As lower and lower frequencies are required, unless the array designer has very large transducer faces, the separation between adjacent radiators will become small compared to the wavelength in water if a high packing factor is to be maintained. A condition of this sort will tend to increase the mutual impedance effects of the array and this is detrimental to velocity control. (cont on p 2) (14) USL-TM-960-47-65

Reference (b) shows that there is a high correlation between lack of velocity control and the occurrence of negative radiation resistances. Negative radiation resistances in an array means that some elements are absorbing power from the rest of the array. Some of this power is dissipated in mechanical and electrical losses in the element, but most of it goes back into the electrical power supply. If many elements are being driven by the same amplifier, then an element returning power to the power supply is merely resupplying electrical power to the other elements. However, the requirement for higher power suggests the use of modular drive, whereby each transducer has its own power supply. In this case the acoustic power absorbed by the element that is not dissipated by internal losses is returned directly to the power supply. If this power becomes excessive, the modular driver may be destroyed.

1-254 200

78 08 07 384

SEP 7 1965

78 08 03 129

UNCLASSIFIED

SECURITY CLASSIFICATION OF THIS PAGE *(When Data Entered)*

REPORT DOCUMENTATION PAGE		READ INSTRUCTIONS BEFORE COMPLETING FORM
1. REPORT NUMBER	2. GOVT ACCESSION NO. 960-47-65	3. RECIPIENT'S CATALOG NUMBER
4. TITLE *(and Subtitle)* BROADBAND VEOLCITY CONTROL		5. TYPE OF REPORT & PERIOD COVERED Tech Memo
		6. PERFORMING ORG. REPORT NUMBER
7. AUTHOR(s) Porter, David T.		8. CONTRACT OR GRANT NUMBER(s) Nonr-266(84)
9. PERFORMING ORGANIZATION NAME AND ADDRESS Naval Underwater Systems Center New London, CT		10. PROGRAM ELEMENT, PROJECT, TASK AREA & WORK UNIT NUMBERS
11. CONTROLLING OFFICE NAME AND ADDRESS Office of Naval Research, Code 220 800 North Quincy St. Arlington, VA 22217		12. REPORT DATE 30 JUN 65
		13. NUMBER OF PAGES
14. MONITORING AGENCY NAME & ADDRESS*(if different from Controlling Office)*		15. SECURITY CLASS. *(of this report)* UNCLASSIFIED
		15a. DECLASSIFICATION/DOWNGRADING SCHEDULE

16. DISTRIBUTION STATEMENT *(of this Report)*

Approved for public release; distribution unlimited.

17. DISTRIBUTION STATEMENT *(of the abstract entered in Block 20, if different from Report)*

18. SUPPLEMENTARY NOTES

19. KEY WORDS *(Continue on reverse side if necessary and identify by block number)*

20. ABSTRACT *(Continue on reverse side if necessary and identify by block number)*

DD FORM 1 JAN 73 1473 EDITION OF 1 NOV 65 IS OBSOLETE
S/N 0102-LF-014-6601

UNCLASSIFIED

SECURITY CLASSIFICATION OF THIS PAGE *(When Data Entered)*

PENNSYLVANIA STATE UNIVERSITY
ORDNANCE RESEARCH LABORATORIES
CONTRACT Nonr-266(84)

Various new techniques are being explored in order to maintain velocity control. Some of these are mechanoelectrical feedback, and the use of series or parallel tuning reactors in conjunction with voltage or current drivers. This report will explore the feasibility of maintaining velocity control over a wide band and will not consider feedback.

The problem will be separated into two parts: array factors (factors external to the transducer), and transducer factors (factors internal to the transducer). This report is mainly concerned with the transducer factors. However, a short dissertation on array factors will be contained herein for familiarization purposes. For the idealized case of a planar, broadside, close-packed array of circular pistons in a rigid baffle, some array factors are discussed in reference (b).

ARRAY FACTORS

Reference (b) discusses Thevenin's equivalent circuit for transducers. Figure (1) shows a Thevenin's equivalent circuit for the jth element in an array.

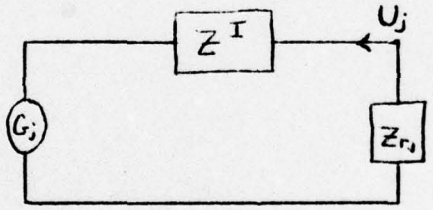

Figure 1.
Thevenin's Equivalent Circuit for an Array Element

G_j is the Thevenin's equivalent input force, Z^I is the Thevenin's equivalent internal impedance, U_j is the velocity of the radiating face, and Z_{rj} is the total radiation impedance. The equation relating these variables is

$$G_j = U_j (Z^I + Z_{rj}), \qquad (1)$$

and Z_{rj} is related to the velocities of the other transducers in the array by

$$Z_{rj} = \sum_{i=1}^{N} Z_{ij} \frac{U_i}{U_j} . \qquad (2)$$

79 08 03 129

78 08 07 384

Reference (b) also introduces a velocity control factor UCF, defined by

$$UCF = \frac{|Z_{ij}|_{max}}{|Z^I + Z_{11}|} \quad (3)$$

In general, the smaller the UCF, the better velocity control is. Z_{11} is the self radiation impedance of the elements, which were taken to be uniform over the array. $|Z_{ij}|_{max}$ is the maximum absolute value of radiation impedance between pistons occurring in the array. Z_{11} and Z_{12} are factors external to the transducer, which depend on the size, shape, separation, orientation, and frequency of the transducers. The Z^I is the internal factor, which is taken to be independent of the transducer velocities and radiation impedances.

From equation (3) it is seen that if the real (R^I) or imaginary (X^I) part of Z^I is very large, then UCF will be small, and velocity control will be good. Neither R^I nor R_{11} can be negative, but they can both be small. X_{11} cannot be negative, but X^I can, so that when $X^I = -X_{11}$, UCF can be very large, and velocity control can be poor. Therefore, the ratio X^I/X_{11} is more important than the X^I value itself.

For the external part of the problem, we may find what values of Z^I are permitted over the frequency band to be used which will not result in negative radiation resistances. In the transducer factors section, it will be shown that R^I is usually not very frequency dependent, so that in the external part, we may assign the appropriate value of R^I and find which values of X^I will result in the occurrence of negative radiation resistances. Figure (2) (taken from reference (b)) shows what values of X^I result in some negative radiation resistances in a large, planar, broadside, unshaded, close-packed array of circular pistons in a rigid baffle, with $R^I = 0$.

Accession For
NTIS GRA&I
DDC TAB
Unannounced
Justification
By
Distribution/
Availability Codes
Dist. | Avail and/or special
A

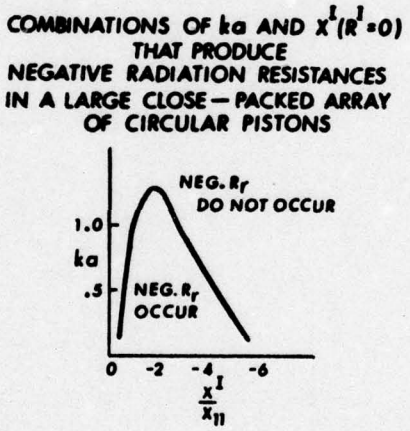

Figure 2.
Occurrence of Negative Radiation Resistances

Had we chosen a larger R^I, or looser packing, the undesirable area in Figure (2) would have been smaller. On the other hand, unequal Z^I or unequal G_j, as might occur due to manufacturing tolerances, would make the undesirable area larger. The undesirable area might also be affected by electrical steering, baffles of different shape (cylindrical, spherical, etc.), and other environmental effects, such as nonrigid baffling and the presence of a dome. The external problem will be considered again at length with more numerical results in a later report.

TRANSDUCER FACTORS

Here we will investigate the effects of various transducer parameters on Z^I, to find out what values of Z^I would actually be encountered over a frequency band. For any array, a diagram, similar to Figure (2), can be made. If the expected values of Z^I do not fall within the undesirable area of this diagram, then presumably negative radiation resistances will not occur in the frequency band to be used.

The following is a list of important factors affecting Z^I:

1. Frequency
2. Power Supply (Voltage or Current Source)
3. Electrical Tuning (Series or Parallel)
4. Coupling Field of the Transducer (Electric Field or Magnetic Field)
5. Effective Coupling Coefficient of the Transducer
6. Front Mass
7. Ratio of Front to Rear Masses
8. Mechanical Resistance Loss (or Mechanical Q in Air)
9. Electrical Resistance in Series with the Power Supply
10. Electrical Conductance in Parallel with the Blocked Reactance

Z^I FOR EIGHT SIMPLE EQUIVALENT CIRCUITS

1. The Results for Eight Cases.

In this section equations will be given for Z^I for the conditions of voltage or current drive, series or parallel tuning, and electric or magnetic field. The circuits considered here consist only of a mechanical resistance, mass and compliance, and electrical blocking and tuning reactances. In the Appendices, the effects on Z^I of adding a rear mass and electrical losses will be considered.

Figure (3) shows the eight equivalent circuits (obtained from reference (c)), equations for their Z^I, and sketches of the frequency dependence of X^I. Note that in these eight cases R^I is just the mechanical resistance, which is assumed here to be frequency independent. In Figures 4a, b, c, d and e, graphs of the quotient X^I/X_{11} are presented which illustrate the dependence of X^I on the effective coupling coefficient. Note also that many of the eight expressions for X^I have the same form, so that in Figure (4) only five graphs were needed instead of eight.

2. Derivation of Z^I for the Voltage Source, Series Tuned, Electric Field Case.

The equation for Z^I for the voltage source, series tuned, electric field

(VSE) case will now be derived. To find Z^I, we first remove the electromechanical transformer from circuit 3a by transferring the electrical impedance to the mechanical side (Figure 5a). Then we short circuit the force source, F = NE, and examine the impedance looking back into the transducer from the radiating face (Figure 5b).

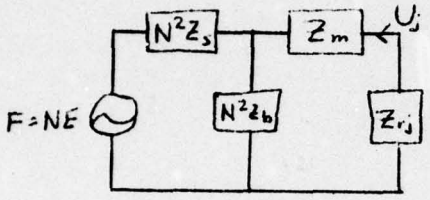

Figure 5a.

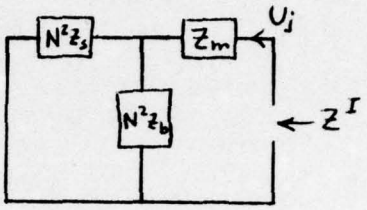

Figure 5b.

Circuits used to find Z^I for the Voltage Source, Series Tuned, Electric Field Case

Here Z_s is the series tuning reactance, Z_b is the blocked reactance, and Z_m is the mechanical impedance. Solving for Z^I, we obtain

$$Z^I = Z_m + \frac{1}{\frac{1}{N^2 Z_s} + \frac{1}{N^2 Z_b}} = Z_m + \frac{N^2 Z_s Z_b}{Z_s + Z_b} . \quad (4)$$

Inserting the proper terms for Z_m, Z_b, and Z_s, we have

$$Z^I = R_m + j\omega M + \frac{1}{j\omega C_m} + \frac{N^2 j\omega L_s \frac{1}{j\omega C_b}}{j\omega L_s + \frac{1}{j\omega C_b}} , \quad (5)$$

so that

$$R^I = R_m , \quad (6)$$

and

$$X^I = \omega M - \frac{1}{\omega C_m} - \frac{N^2 L_s / C_b}{\omega L_s - \frac{1}{\omega C_b}} \quad . \tag{7}$$

$\left(N^2 \frac{\omega L_s}{\omega^2 C_b L_s - 1}\right)$ or also $\left(N^2 \frac{1}{\omega C_b - \frac{1}{\omega L_s}}\right)$

Let us define a reference angular frequency ω_o, such that

$$\omega_o \equiv \frac{1}{\sqrt{M C_m}} \quad . \tag{8a}$$

This ω_o will correspond to the mechanical resonant frequency in air with the source voltage held constant, and with no tuning reactance in the circuit. Now we choose the tuning inductor such that tuning reactance cancels the blocked reactance at ω_o. Then we have

$$\omega_o = \frac{1}{\sqrt{L_s C_b}} = \frac{1}{\sqrt{M C_m}} \quad . \tag{8b}$$

After some algebra,

$$X^I = \omega_o M \left[\frac{\left(\frac{\omega}{\omega_o}\right)^2 - 1}{\omega/\omega_o} \right] + \frac{\omega}{\omega_o} \frac{N^2}{\omega_o C_b \left(1 - \left(\frac{\omega}{\omega_o}\right)^2\right)} \quad . \tag{9}$$

For constant voltage drive, we may relate C_b and C_m by

$$\frac{N^2 C_m}{C_b} = \frac{k_e^2}{1 - k_e^2}, \tag{10}$$

where k_e is the effective coupling coefficient of the transducer. We may eliminate C_m by use of equation (8), so that finally

$$\frac{X^I}{\omega_o M} = \frac{\left(\frac{\omega}{\omega_o}\right)^2 - 1}{\frac{\omega}{\omega_o}} - \frac{\frac{\omega}{\omega_o}\frac{k_e^2}{1-k_e^2}}{\left(\frac{\omega}{\omega_o}\right)^2 - 1}. \tag{11}$$

We now express the self radiation reactance X_{11} by

$$X_{11} = \omega M_r, \tag{12}$$

where M_r is the self radiation mass, which can be considered constant when the frequencies are such that the piston face is small relative to a wavelength. For circular pistons of small ka in a rigid baffle, X_{11} is $(8/3\pi)ka\rho cA$, so that M_r is $\frac{8}{3}\rho a^3$.

Now the ratio of X^I to X_{11} becomes

$$\frac{X^I}{X_{11}} = \frac{M}{M_r}\left[\frac{\left(\frac{\omega}{\omega_o}\right)^2 - 1}{\left(\frac{\omega}{\omega_o}\right)^2} - \frac{\frac{k_e^2}{1-k_e^2}}{\left(\frac{\omega}{\omega_o}\right)^2 - 1}\right]. \tag{13}$$

From (13), it is seen that $X^I/X_{11} \to \infty$ at $\omega = \omega_o$. To find the zero crossings of X^I/X_{11}, we first set $\frac{k_e^2}{1-k_e^2} = C_1$, and $\frac{\omega}{\omega_o} = \beta$.

Then we have

$$\frac{X^I}{X_{11}} = \frac{M}{M_r}\left[\frac{\beta^2-1}{\beta^2} - \frac{C_1}{\beta^2-1}\right]. \tag{14}$$

For $X^I = 0$,

$$\frac{\beta^2-1}{\beta^2} = \frac{C_1}{\beta^2-1}, \tag{15}$$

and

$$(\beta^2-1)^2 = C_1\beta^2, \tag{16}$$

so that

$$\beta^2 - 1 \pm \beta\sqrt{C_1} = 0, \tag{17}$$

which has the solution

$$\beta = \pm\frac{\sqrt{C_1} \pm \sqrt{C_1+4}}{2}, \tag{18}$$

which can be approximated by

$$\beta \approx 1 \pm \frac{\sqrt{C_1}}{2} \quad , \text{for } \sqrt{C_1} \ll 1 \tag{19}$$

and

$$\omega_{\substack{\text{zero}\\\text{crossing}}} \approx \omega_o\left(1 \pm \frac{k_e}{2}\right) \qquad (20)$$

GENERALIZATIONS CONCERNING X^I FOR THE EIGHT SIMPLE EQUIVALENT CIRCUITS

1. Effect of Type of Field

The choice of electric or magnetic field had little effect on the graphs of X^I/X_{11} versus ω/ω_o. The only noticeable effect was in the unimportant case of current drive with series tuning (ISE, ISM cases), where the zero crossing is affected differently by coupling coefficient in the ISE case than in the ISM case.

2. Effects of type of Drive and Tuning

The cases of voltage drive with series tuning and current drive with parallel tuning have X^I curves of the same form, with a pole at $\omega = \omega_o$, and zero crossings at about $\omega/\omega_o = 1 \pm k_e/2$.

The cases of voltage drive with parallel tuning and current drive with series tuning have X^I curves of the same form, with no poles, and a zero crossing at or near $\omega = \omega_o$.

3. Effects of Coupling Coefficient

In the VS and IP cases, increasing the coupling coefficient makes the absolute value of X^I greater in the vicinity of $\omega = \omega_o$, and also increases the frequency separation between the zero crossings, effects which are both advantageous for increasing the bandwidth over which velocity control may obtained. The VP cases are independent of coupling coefficient, and the zero crossing is at $\omega = \omega_o$. In the ISE case, the frequency of the zero crossing is increased by increasing coupling coefficient, while in the ISM case the frequency of the zero crossing is reduced by increasing coupling coefficient. This results in the ISM case having a positive X^I at $\omega = \omega_o$, which is beneficial to velocity control, (see Figure 2), and in the ISE case having a negative X^I at $\omega = \omega_o$, which is bad for velocity control. The ISE and ISM cases are mostly of academic interest, as transducers are seldom designed in such a manner. However, these two cases are of interest in considering series tuned transducers which have high source impedances.

4. Effects of Changing the Tuning Reactor

The X^I curves for the VPE and VPM cases are unaffected by the tuning reactor, so that changing the tuning reactor will not affect these cases. In the VSE, VSM, IPE and IPM cases, the pole occurs when the tuning reactance cancels the blocked reactance, Therefore, changing the tuning reactor changes the frequency at which the pole occurs. The X^I curves for the ISE and ISM cases are independent of the series tuning reactor, so that changing the reactor does not affect the ISE or ISM X^I curves.

5. Effects of Changing the Ratio of Front Mass to Self Radiation Mass (M/M_r)

For all cases, the ratio of X^I/X_{11} is directly proportional to M/M_r, so that increasing M/M_r increases the magnitude of X^I/X_{11}, which is generally beneficial to velocity control. However, this is a poor way to obtain velocity control, for two reasons, namely, (a) raising M raises the mechanical Q which forces a redesign of the transducer; and (b) reducing M_r implies using a smaller transducer face, which means a smaller ka of the radiating face, which in turn makes velocity control harder.

A SIMPLE EXAMPLE OF BROADBAND VELOCITY CONTROL

Consider a large, close-packed, broadside array of circular pistons in a rigid baffle. Let $M/M_r = 4$, $R^I = 0$, the coupling coefficient be 44.7%, the piston diameters be eight (8) inches, and the resonant frequency in air $f_o = \frac{\omega_o}{2\pi}$ be 1 k.c. Let the array be series tuned, so that it can be described by circuit 3a. Recalling that the wave number k can be expressed as $\omega/c = 2\pi f/c$, and assuming c = 5000 feet/second in water, the ka of the pistons will be 0.424 at 1 k.c. Now, ka and ω/ω_o are related by

$$ka = 0.424\ \omega/\omega_o \qquad (21)$$

This enables us to plot the undesirable operating area from Figure (2) and the actual ratio of X^I/X_{11} from Figure (4a) on the same graph, as is shown in Figure (6). For series tuning, the ratio X^I/X_{11} will be such as to result in some negative radiation resistances for frequencies between 625 cps and 750 cps and also between 1100 cps and 1225 cps. Therefore, the velocity control obtained between 750 cps and 1100 cps is sufficient to avoid negative radiation resistances, and we may call the velocity control bandwidth of this transducer 350 cycles.

AN EXAMPLE OF BROADBAND VELOCITY CONTROL

Undesirable area in graph is where some pistons absorb power from the array.
Large unsteered, planar array of circular pistons is considered.
Resonant frequency in air: 1 k.c.
Piston diameter: eight (8) inches
Coupling coefficient: 0.447
Electric field
Voltage source
Tuning reactance cancels blocked reactance at 1 k.c.
Piston ka at 1 k.c.: 0.424
Ratio of moving mass to radiation mass: 4:1
The undesirable area is taken from Figure (2).
The actual ratios X^I/X_{11} are taken from Figures (4a) and (4b).
For series tuning the undesirable frequencies are 625 cps to 750 cps and 1100 cps to 1225 cps.
For parallel tuning undesirable frequencies are from 680 cps to 950 cps.

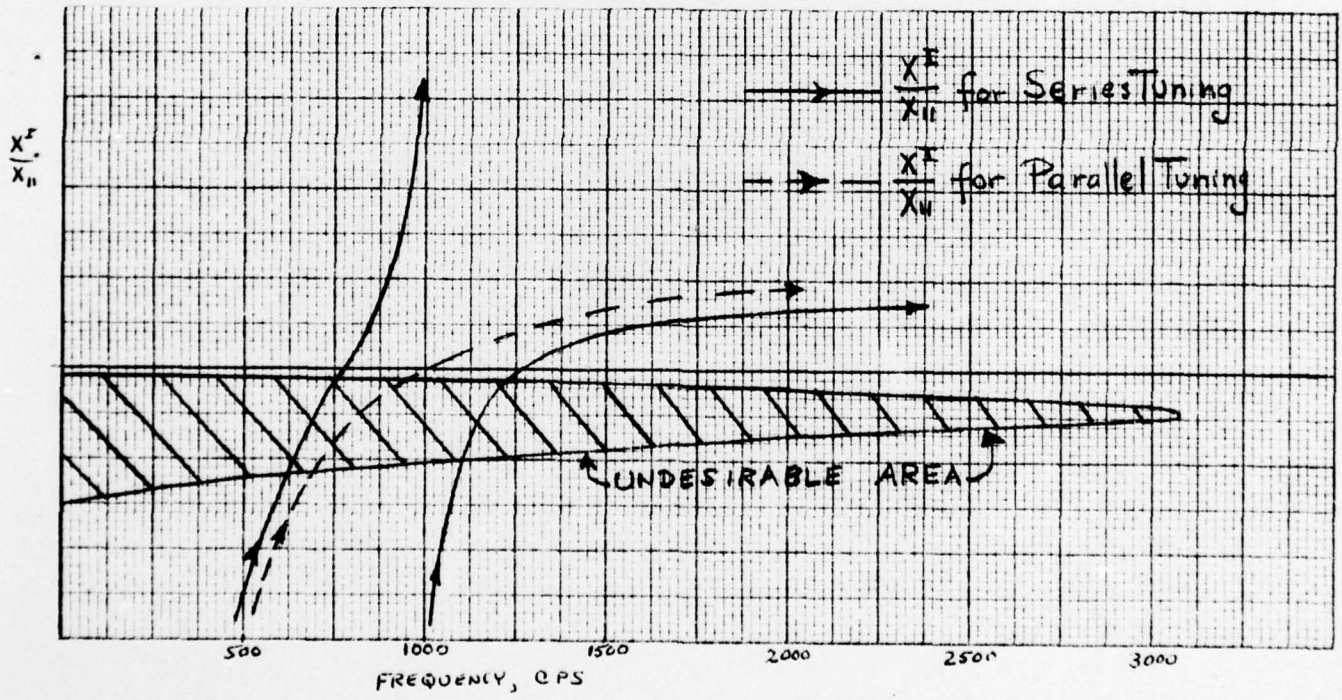

Figure 6.

We now change the tuning of this array to parallel tuning. Then some elements would have negative radiation resistances for frequencies between 680 cps and 950 cps. However, as we further increase the frequency, there would be no upper frequency at which negative radiation resistances would reoccur, and we cannot assign a velocity control bandwidth to this parallel-tuned array. Although negative radiation resistances do not occur at the resonant frequency in air, they do occur only 50 cps lower, so that the resonant frequency in water of the parallel-tuned array probably does lie in the undesirable area.

DAVID T. PORTER
Mathematician

LIST OF REFERENCES

(a) D. L. Carson,"Diagnosis and Cure of Erratic Velocity Distributions in Sonar Projector Arrays", Journal of the Acoustical Society of America, Vol. 34, pp. 1191-1196, 1962.

(b) D. T. Porter, "Effect of Thevenin Equivalent Internal Impedance on Velocity Control and Acoustic Power of Planar Broadside Arrays for Different Level Limitations", USL Report No. 648, 28 April 1965.

(c) R. S. Woollett, Lecture Notes on Sonar Transducer Fundamentals.

APPENDIX A

Here we consider the effect on Z^I of adding a rear mass to the circuit in Figure (3a) for the VSE case. In Figure (A-1), the front and rear masses are denoted by M_1 and M_2.

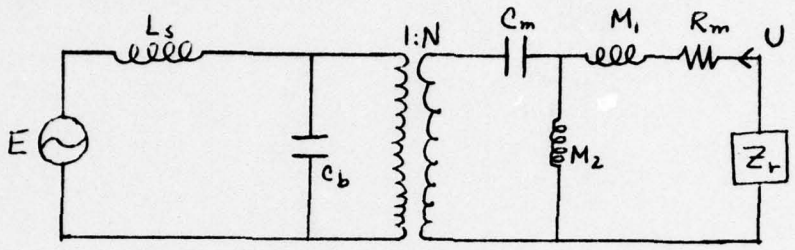

Figure A-1.
Addition of Rear Mass to Circuit 3a (VSE Case)

For the circuit in Figure (A-1), we define a new reference frequency

$$\omega_o \equiv \frac{1}{\sqrt{\frac{M_1 M_2}{M_1 + M_2} C_m}} \qquad \text{(A-1)}$$

This ω_o will correspond to the mechanical resonant frequency in air with the source voltage held constant, no tuning reactance in the circuit, and no losses in the circuit. (The presence of the tuning reactance and some losses will affect the resonant frequency only slightly.

To find Z^I for the circuit of Figure (A-1), we short circuit the voltage source, and look back in from the radiating face, as is shown in Figure (A-2).

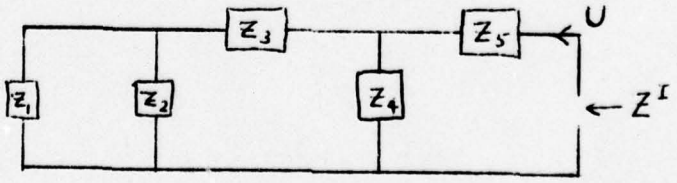

Figure A-2
Finding Z^I for the Circuit of Figure A-1

Setting

$$Z_6 = \frac{Z_1 Z_2}{Z_1 + Z_2} \tag{A-2}$$

$$Z_7 = Z_3 + Z_6 \tag{A-3}$$

$$Z_8 = \frac{Z_4 Z_7}{Z_4 + Z_7} \tag{A-4}$$

we find that

$$Z^I = Z_5 + Z_8 = Z_5 + \frac{1}{\frac{1}{Z_4} + \frac{1}{Z_3 + \frac{Z_1 Z_2}{Z_1 + Z_2}}} \; . \tag{A-5}$$

Now we define

$$\begin{aligned} \omega_1 &\equiv \frac{1}{\sqrt{L_5 C_6}} \\ \alpha &\equiv \omega/\omega_1 \\ s &\equiv M_1/M_2 \\ C_1 &\equiv \frac{k_e^2}{1-k_e^2} \; . \end{aligned} \tag{A-6}$$

When we put the appropriate circuit parameters into (A-5) and make use of the definitions in (A-6), we obtain

$$R^I = r_m \tag{A-7}$$

and

$$X^I = \omega M_1 \left[1 + \frac{1}{s - \left(\frac{\omega_1}{\omega_0}\right)^2 (s+1) \frac{\alpha^2 - 1}{C_1 + \frac{\alpha^2 - 1}{\alpha^2}}} \right] . \tag{A-8}$$

COLUMBIA UNIVERSITY
HUDSON LABORATORIES
CONTRACT Nonr-266(84)

Suppose now that we want X^I to be very large at ω_o, so that velocity control will be obtained for frequencies near mechanical resonance. Assume that we are not free to alter the transducer proper, but that we may adjust the tuning coil. Then we must find the proper value of $\omega_1 = 1/\sqrt{L_s C_b}$, such that X^I approaches infinity at $\omega = \omega_o$. X^I will be infinite if the denominator in the fraction of (A-8) is zero. As we want this denominator to be zero when $\omega = \omega_o$, we set $\alpha = \omega_o / \omega_1$, and seek a solution of

$$s = \frac{1}{\alpha^2}(s+1)\frac{\alpha^2 - 1}{C_1 + \frac{\alpha^2 - 1}{\alpha^2}} \quad . \tag{A-9}$$

When the algebra is done, we find simply

$$\omega_1 = \omega_o \sqrt{1 - C_1 s} \quad . \tag{A-10}$$

As $C_1 s \ll 1$, we can approximate (A-10) by

$$\omega_1 \approx \omega_o \left(1 - \frac{C_1 s}{2}\right) \tag{A-11}$$

Equation (A-11) shows us that the proper tuning coil is almost exactly the same as would be required if the circuit in Figure (A-1) did not include a rear mass, or had an infinite rear mass. Consider a sample case where $M_1/M_2 = 1/3 = s$, and $k_e = 1/3$. Then $C_1 = 1/8$, and $\omega_1 = \omega_o\ (1 - 1/48)$.

When the zero crossings of the X^I in (A-8) are found, (having chosen ω_1 from (A-10)), it is seen that they lie at almost the same frequencies as for the simpler circuit 3a with no rear mass in it. However, for zero frequency, X^I is now zero.

The most interesting effect of the rear mass on X^I is that there is now another pole, or perhaps we should say that the pole that was at zero frequency has moved to a greater frequency. Upon putting (A-10) into (A-8)

and finding what frequencies give a zero denominator in (A-8), we find that

$$\frac{\omega}{\omega_1} = \left\{ \begin{array}{l} \dfrac{1}{\sqrt{1-C_1 s}} \\ \sqrt{s/(1+s)} = \sqrt{\dfrac{M_1}{M_1+M_2}} \end{array} \right\} \qquad \text{(A-12)}$$

The first root in (A-12) is just the already established pole at ω_o, given by (A-10), but the second is a low frequency pole. For $s = M_1/M_2 = 1/3$, this pole lies at $\omega/\omega_1 = 1/2$, and the X^I curve has the form shown in Figure (A-3).

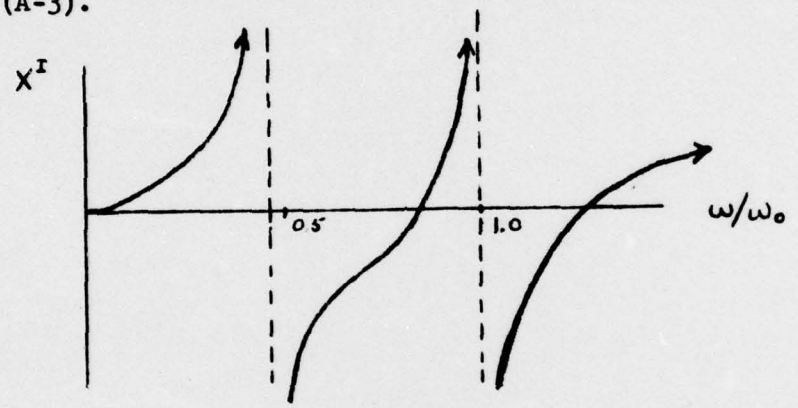

Figure A-3
X^I Curve for a Front to Rear Mass Ratio of 1/3 (VSE Case)

The parallel tuned case (VPE) also has a low frequency pole, which is determined by the parallel resonance of C_m and M_2. It can be shown that X^I approaches infinity for $\omega = \omega_o\sqrt{s/(1+s)}$. The X^I curve for the VPE case is shown in Figure (A-4).

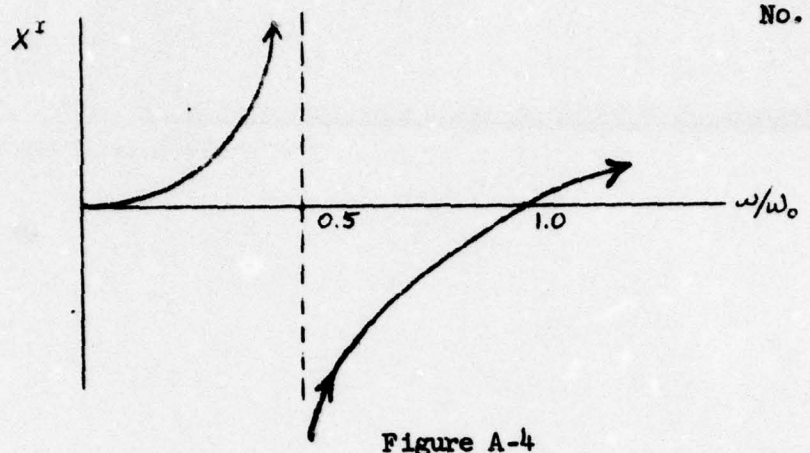

Figure A-4
X^I Curve for a Front to Rear Mass Ratio of 1/3 (VPE)

APPENDIX B

ADDITION OF AN ELECTRICAL LOSS, G_b, IN PARALLEL WITH THE BLOCKED REACTANCE

Here we consider the effect on Z^I of adding an internal loss G_b to the basic circuit of Figure (3a) for the VSE case. This loss is shown in Figure B-1.

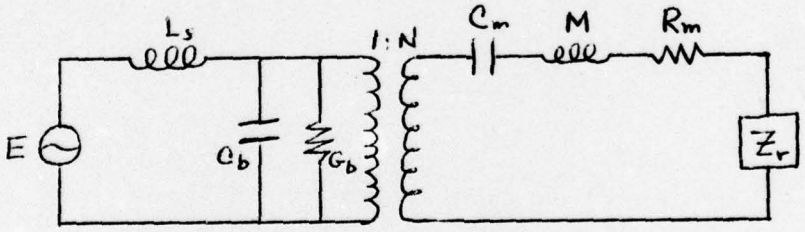

Figure B-1
Addition of G_b to Circuit 3a (VSE Case)

Still assuming the resonances of M and C_m, and also L_s and C_b to be at $\omega = \omega_o$, the Z^I can be shown to be

$$Z^I = R_m + j\omega M\left(1-\left(\frac{\omega_o}{\omega}\right)^2\right) + \frac{N^2}{G_b + j\omega C_b\left(1-\left(\frac{\omega_o}{\omega}\right)^2\right)} \qquad \text{(B-1)}$$

which at $\omega = \omega_0$ reduces to

$$R^I = R_m + \frac{N^2}{G_b}, \quad X^I = 0. \tag{B-2}$$

Note that we have lost the pole at $\omega = \omega_0$, but R^I may still be very large if N^2/G_b is large. Indeed, as G_b approaches 0, R^I approaches infinity, and complete velocity control is established, just as in the case when we did not take G_b into account. It will be convenient now to assume that G_b is linearly frequency dependent, such that tan δ remains fairly constant over a wide frequency range. Tanδ is given by

$$\tan\delta \equiv \frac{G_b}{B_b} = \frac{G_b}{\omega C_b} \tag{B-3}$$

Then it can be shown that

$$R^I = R_m + \frac{\omega_0 M}{\omega/\omega_0} \frac{k_e^2}{1-k_e^2} \frac{\tan\delta}{\left(1-\left(\frac{\omega_0}{\omega}\right)^2\right)^2 + \tan^2\delta} \tag{B-4}$$

and

$$X^I = \omega M\left(1-\left(\frac{\omega_0}{\omega}\right)^2\right) - \frac{\omega_0 M}{\omega/\omega_0} \frac{k_e^2}{1-k_e^2} \frac{1-\left(\frac{\omega_0}{\omega}\right)^2}{\left(1-\left(\frac{\omega_0}{\omega}\right)^2\right)^2 + \tan^2\delta}. \tag{B-5}$$

Sketches of R^I and X^I versus frequency are shown in Figure B-2.

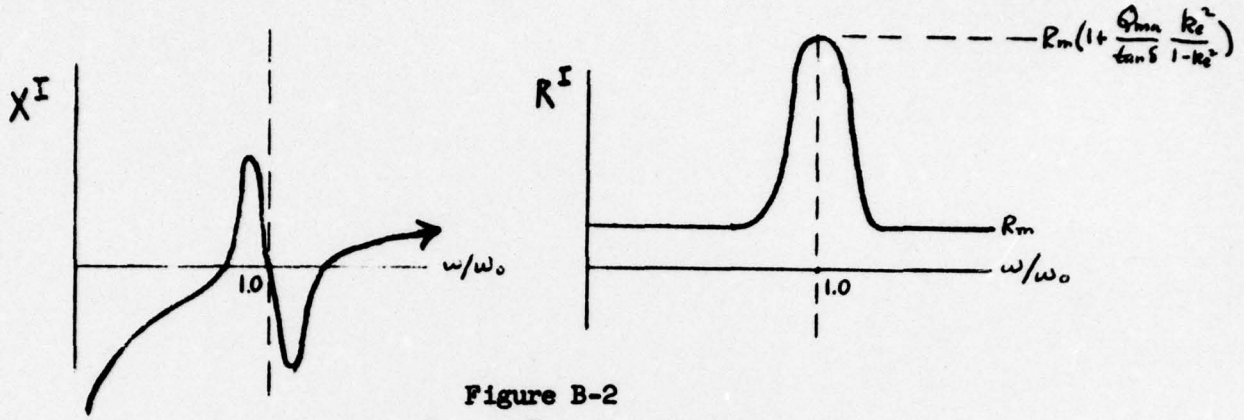

Figure B-2

Effect on R^I and X^I of G_b for VSE Case

Then at $\omega=\omega_o$ R^I becomes

$$R^I = R_m + \omega_o M \frac{k_e^2}{1-k_e^2} \frac{1}{\tan\delta} = R_m\left(1+\frac{Q_{ma}}{\tan\delta}\frac{k_e^2}{1-k_e^2}\right) \qquad \text{(B-6)}$$

or,

$$\frac{R^I}{X_{11}} = \frac{M}{M_r}\left[\frac{R_m}{\omega_o M} + \frac{k_e^2}{(1-k_e^2)\tan\delta}\right] \qquad \text{(B-7)}$$

Just as in the case when we did not consider G_b ($\tan\delta = 0$), the magnitude of Z^I and the resulting degree of velocity control are very dependent upon the coupling coefficient. If the electrical part of the transducer circuit is weakly coupled to the mechanical part, then the high impedance of the tank circuit made by L_s and C_b will only give a small effect to Z^I.

The analysis contained in equations (B-1) through (B-7) is also pertinent to the case of a current source with parallel tuning. Z^I for the cases of voltage source and parallel tuning (VPE, VPM) is not affected by G_b.

APPENDIX C

ADDITION OF AN ELECTRICAL LOSS, R_1, IN SERIES WITH THE TRANSDUCER

1. 1. VSE Case

Now we alter circuit 3a by adding a resistance R_1 in series with the tuning coil. This resistance may be considered as either a source impedance or an electrical loss internal to the coil or transducer.

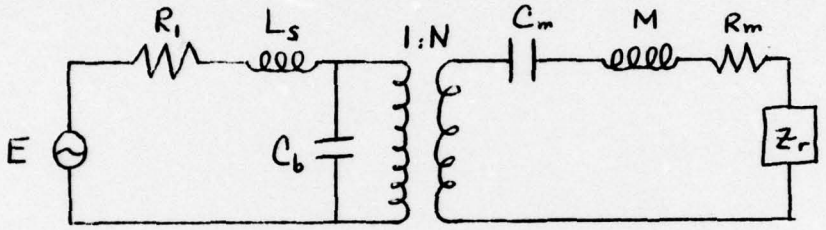

Figure C-1
Addition of Series Resistance to Circuit 3a (VSE Case)

Now Z^I can be shown to be

$$Z^I = R_m + j\omega_o M \frac{(\omega/\omega_o)^2 - 1}{\omega/\omega_o} + \frac{k_e^2}{1-k_e^2}\omega_o M \frac{\frac{\omega_o L_s}{R_1} - j\frac{\omega_o}{\omega}}{1 - j\frac{\omega_o L_s}{R_1}\left(\frac{1-(\omega/\omega_o)^2}{\omega/\omega_o}\right)} \qquad \text{(C-1)}$$

Defining

$$Q_1 \equiv \frac{\omega_o L_s}{R_1} \qquad \text{(C-2)}$$

we get

$$Z^I = R_m + j\omega_o M \frac{(\omega/\omega_o)^2 - 1}{\omega/\omega_o} + \frac{k_e^2}{1-k_e^2}\omega_o M \frac{Q_1 - j\frac{\omega_o}{\omega}}{1 - jQ_1\left(\frac{1-(\omega/\omega_o)^2}{\omega/\omega_o}\right)} \qquad \text{(C-3)}$$

If the Z^I of (C-3) were separated into R^I and X^I, then the R^I and X^I would appear as in the sketch in Figure (C-2), which is similar to B-2, which accounted for the G_b loss.

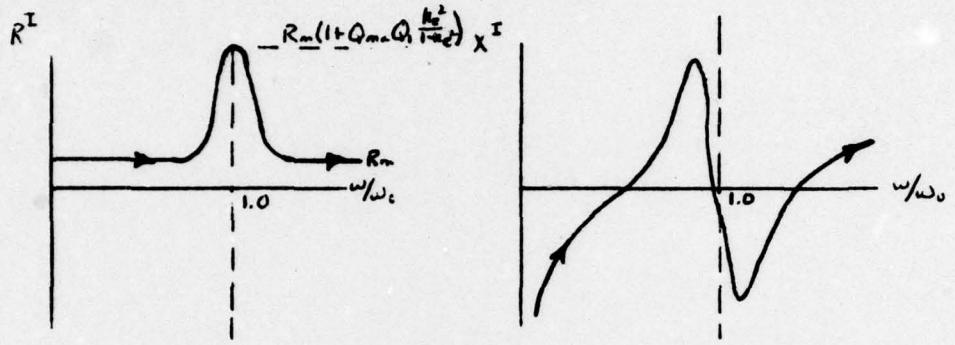

Figure C-2
Effect on R^I and X^I of Series Loss R_1 for VSE Case

When $\omega = \omega_o$, then R^I and X^I simplify to

$$R^I = R_m + \frac{k_e^2}{1-k_e^2}\,\omega_o M Q_1 \qquad \text{(C-4)}$$

and

$$X^I = -\frac{k_e^2}{1-k_e^2}\,\omega_o M \qquad \text{(C-5)}$$

Note that as R_1 becomes larger, Q_1 becomes smaller, and R^I for $\omega = \omega_o$ also becomes smaller, and the velocity control becomes poorer. On the other hand, as R_1 becomes smaller, R^I approaches infinity, and complete velocity control is established.

2. VPE Case

If we add a series resistance R_1 to the original VPE circuit, Figure (3b),

we now obtain Figure (C-3).

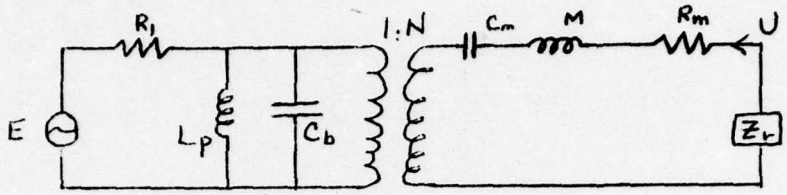

Figure C-3
Addition of Series Resistance to Circuit 3b (VPE Case)

Z^I now becomes

$$Z^I = R_m + j\omega M + \frac{1}{j\omega C_m} + N^2 \frac{jR_1 \frac{\omega L_p}{1-(\omega/\omega_o)^2}}{R_1 + \frac{j\omega L_p}{1-(\omega/\omega_o)^2}} \quad . \tag{C-6}$$

If R_1 becomes very large, the voltage source in conjunction with the large R_1 acts like a current source, and we have the IPE Case again. From Figure (4-a) we see that the IPE case has a pole at $\omega = \omega_o$, which makes the velocity control good. Therefore, addition of a series loss to the VPE case is beneficial to velocity control at $\omega = \omega_o$. Usually, internal electrical losses hurt velocity control, but this case is an exception.

When $\omega = \omega_o$, we have

$$R^I = R_m + N^2 R_1 \tag{C-7}$$

and

$$X^I = 0 \quad . \tag{C-8}$$

After some more algebra it can be shown that at $\omega = \omega_o$

$$R^I = R_m + \frac{k_e^2}{1-k_e^2} \omega_o M \frac{R_1}{\omega_o L_p} = R_m + \frac{k_e^2}{1-k_e^2} \frac{\omega_o M}{Q_1} \tag{C-9}$$

$$= R_m \left(1 + \frac{Q_{mn}}{Q_1} \frac{k_e^2}{1-k_e^2}\right)$$

where

$$Q_1 = \frac{\omega_o L_p}{R_1} = \frac{1}{\omega_o C_b R_1} \quad . \qquad \text{(C-10)}$$

Now let us compare R^I at $\omega = \omega_o$ for the series tuned case (C-4) and the parallel case (C-9). From these two equations we see that velocity control at $\omega = \omega_o$ is better in the series tuned case if Q_1 is greater than 1.0, but is better in the parallel tuned case if Q_1 is less than 1.0. Therefore, if the series resistance R_1 is less than the reactance of the tuning coil (or the blocked reactance of C_b), then at $\omega = \omega_o$ series tuning gives better velocity control, while if R_1 is greater than the tuning reactance at $\omega = \omega_o$, then parallel tuning yields better velocity control.

APPENDIX D

DERIVATION OF X^I EQUATIONS FOR MAGNETIC FIELD CASES

Figure (D-1) shows a simplified two-port circuit for a magnetic field transducer with no tuning reactor (Figure 3d), page 52, Reference (c)).

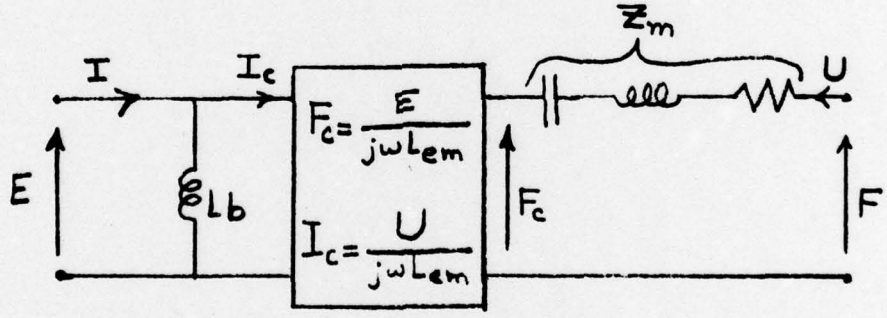

Figure D-1
Two-Port Circuit for Magnetic Field Transducer

The equations relating E, I, F, and U are:

$$F = \frac{1}{j\omega L_{em}} E + Z_m U \qquad \text{(D-1)}$$

and

$$I = Y_b E + \frac{1}{j\omega L_{em}} U. \qquad \text{(D-2)}$$

THIS PAGE IS BEST QUALITY PRACTICABLE
FROM COPY FURNISHED TO DDC

To find Z^I we look back into the transducer from the radiating face, so that

$$Z^I = \frac{F}{U}, \qquad \text{(D-3)}$$

with E = 0 for the voltage source case, and I = 0 for the current source case. And so, for the voltage source case, $Z^I = Z_m$. For the current source case, we first use (D-2) to find

$$E = -\frac{Z_b}{j\omega L_{em}} U, \qquad \text{(D-4)}$$

and put this result into (D-1) to obtain

$$Z^I = \frac{F}{U} = \frac{Z_b}{\omega^2 L_{em}^2} + Z_m \qquad \text{(D-5)}$$

If a parallel tuning capacitor C_p is used, then Z_b will be the parallel combination of C_p and L_b. If a series tuning capacitor C_s is used, then we must replace E by $E - I/j\omega C_s$ in (D-1) and (D-2).

When we define the coupling coefficient by

$$k_e^2 = \frac{L_b C_m}{L_{em}^2} \qquad \text{(D-6)}$$

then the X^I functions for Figures 3e, f, g, and h may be derived by algebra similar to the derivation of 3a.

FIGURES 3a,b,c,d,e,f,g,h
SUMMARY OF Z^I FOR EIGHT SIMPLE CIRCUITS

Case	Designation	Power Source	Tuning	Field	Equivalent Circuit	$X^I/\omega_0 M$ $[\beta = \omega/\omega_0]$	X^I Graph	For a detailed graph of X^I/X_{11} see figure:
a	VSE	Voltage	Series	Electric	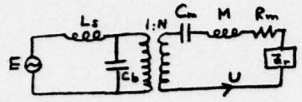	$\frac{\beta^2-1}{\beta} - \frac{C_1}{\frac{\beta^2-1}{\beta}}$	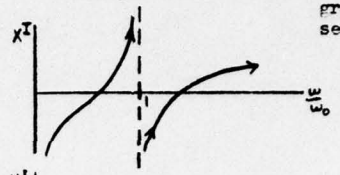	4a
b	VPE	Voltage	Parallel	Electric	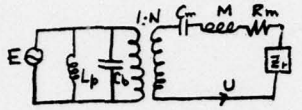	$\frac{\beta^2-1}{\beta}$	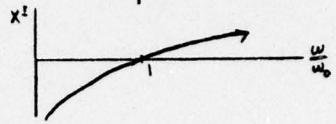	4b
c	ISE	Current	Series	Electric	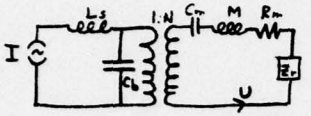	$\frac{\beta^2-1}{\beta} - \frac{C_2}{\beta}$	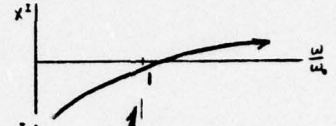	4c
d	IPE	Current	Parallel	Electric	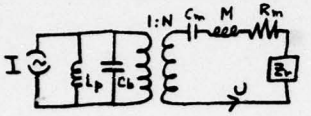	$\frac{\beta^2-1}{\beta} - \frac{C_2}{\frac{\beta^2-1}{\beta}}$		4a
e	VSM	Voltage	Series	Magnetic	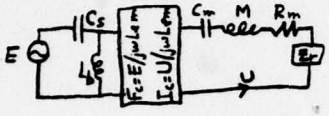	$\frac{\beta^2-1}{\beta} - \frac{C_2}{(\beta^2-1)\beta}$	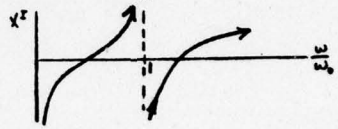	4d
f	VPM	Voltage	Parallel	Magnetic	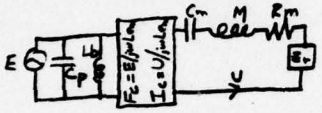	$\frac{\beta^2-1}{\beta}$	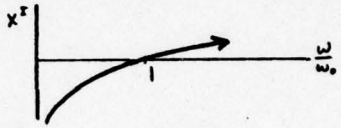	4b
g	ISM	Current	Series	Magnetic	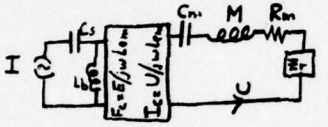	$\frac{\beta^2-1}{\beta} + \frac{C_1}{\beta}$	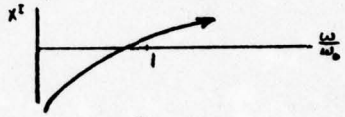	4e
h	IPM	Current	Parallel	Magnetic	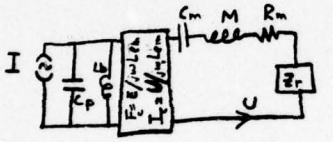	$\frac{\beta^2-1}{\beta} - \frac{C_1}{(\beta^2-1)\beta}$	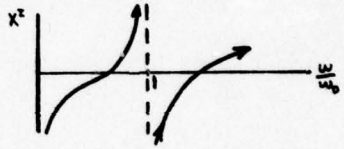	4d

Note: $\omega_0 \equiv \frac{1}{\sqrt{MC_m}}$ and the tuning reactance cancels the blocked reactance at $\omega = \omega_0$.

Note: $R^I = R_m$ for the 8 cases (a) through (h).
$C_1 = \frac{k_e^2}{1-k_e^2}$
$C_2 = k_e^2$

THIS PAGE IS BEST QUALITY PRACTICABLE
FROM COPY FURNISHED TO DDC

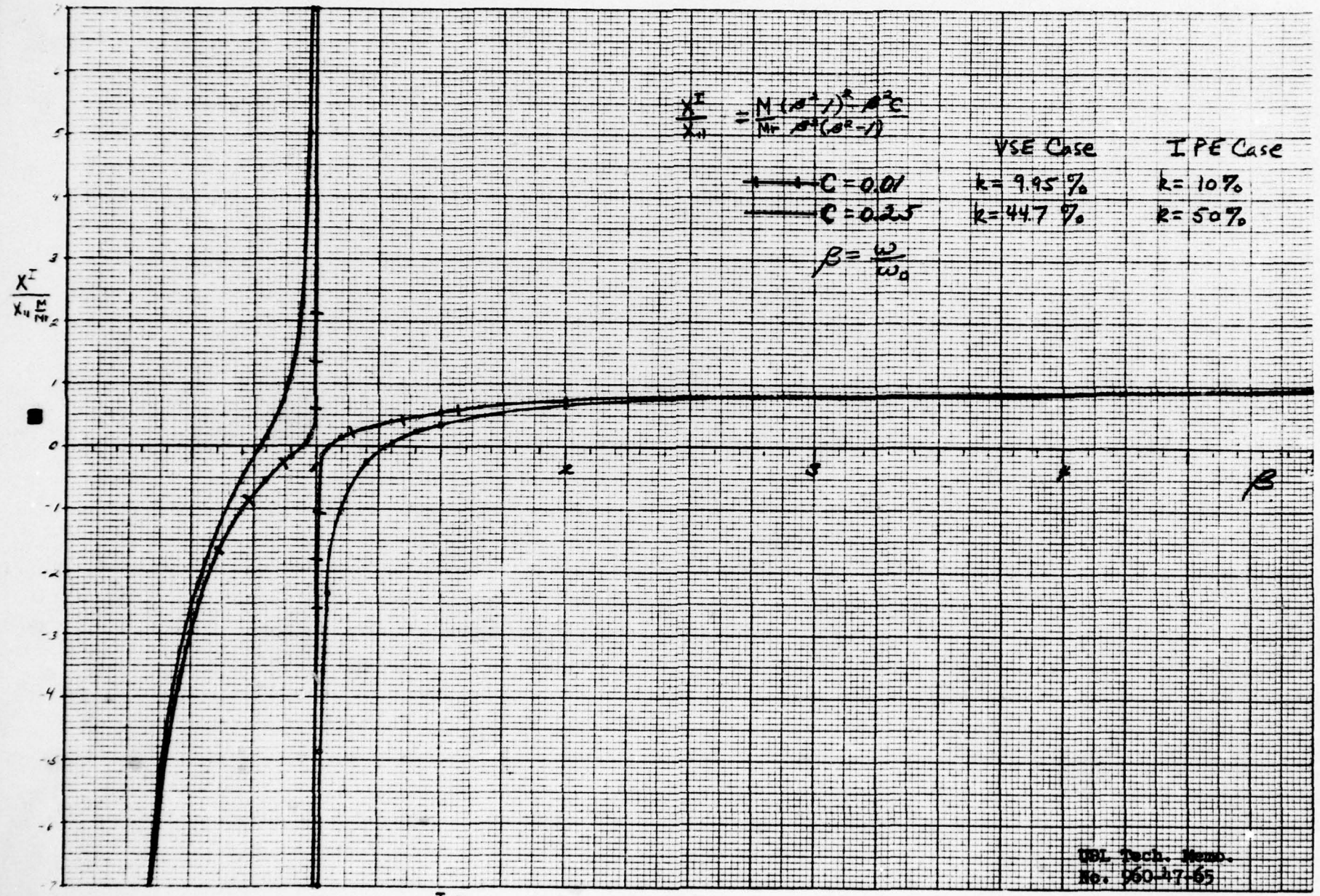

Figure 4a X^I/X_{11} for VSE and IPE Cases

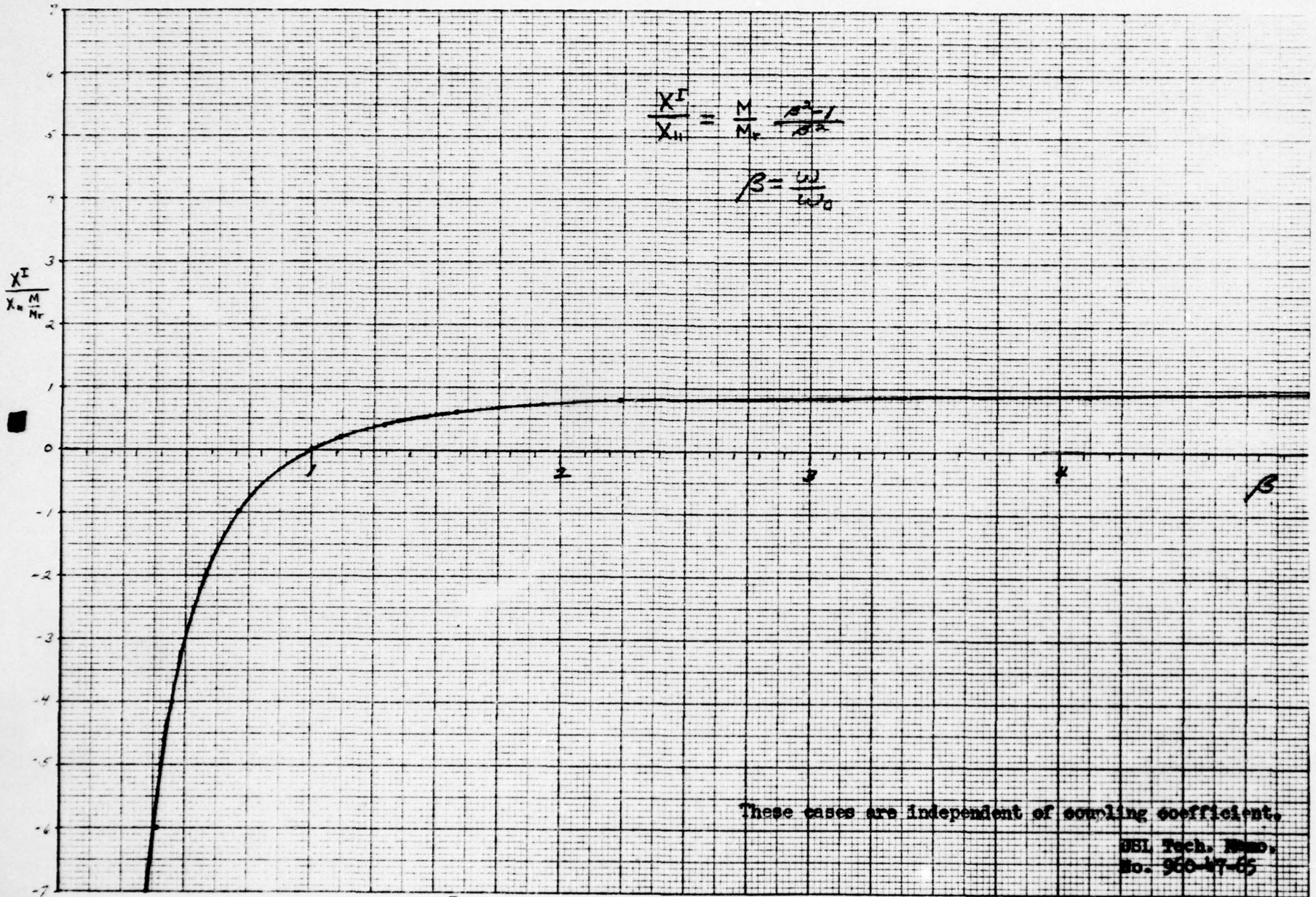

Figure 4b X^I/X_{11} for VPE and VPI Cases

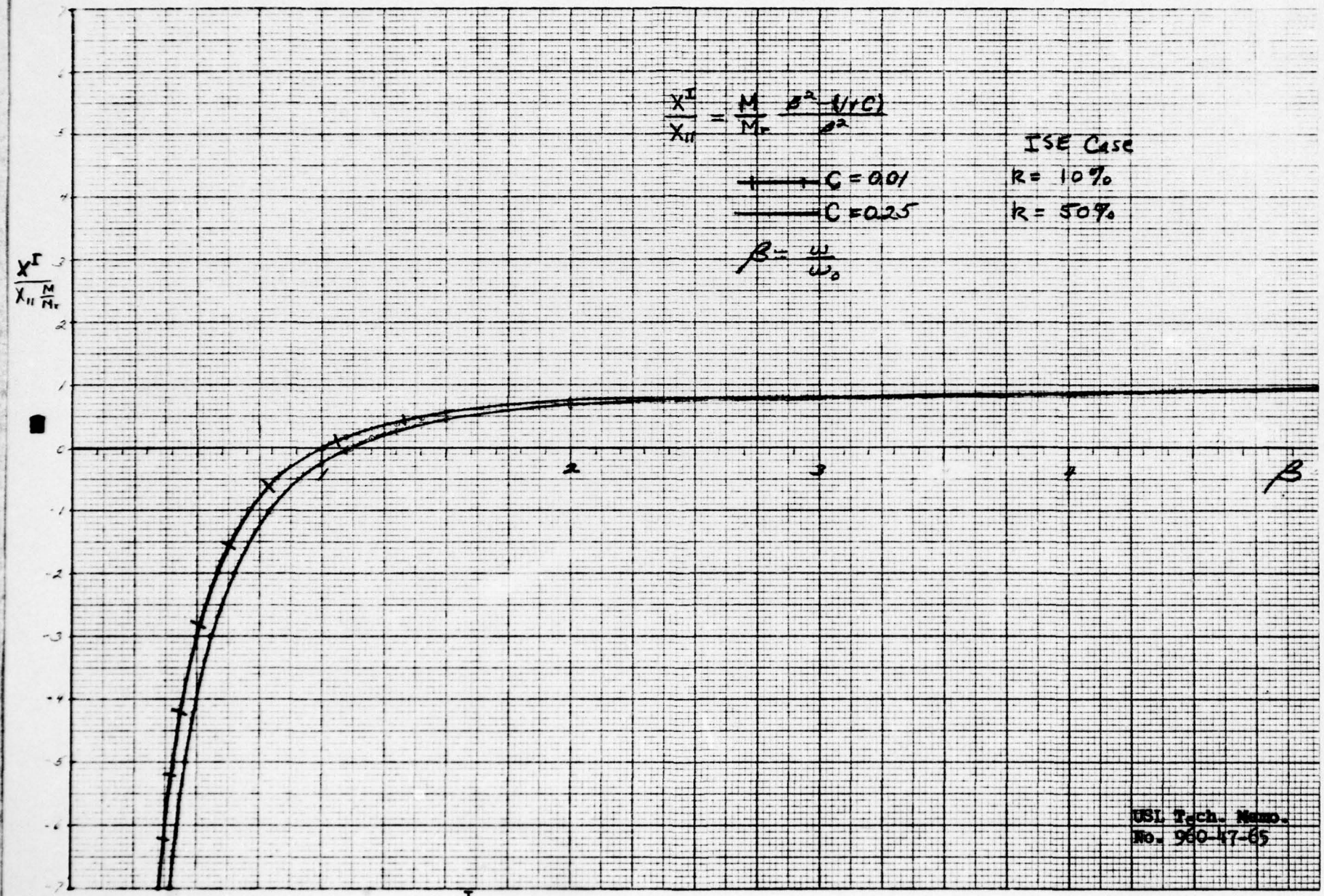

Figure 4c X^I/X_{II} for ISE Case

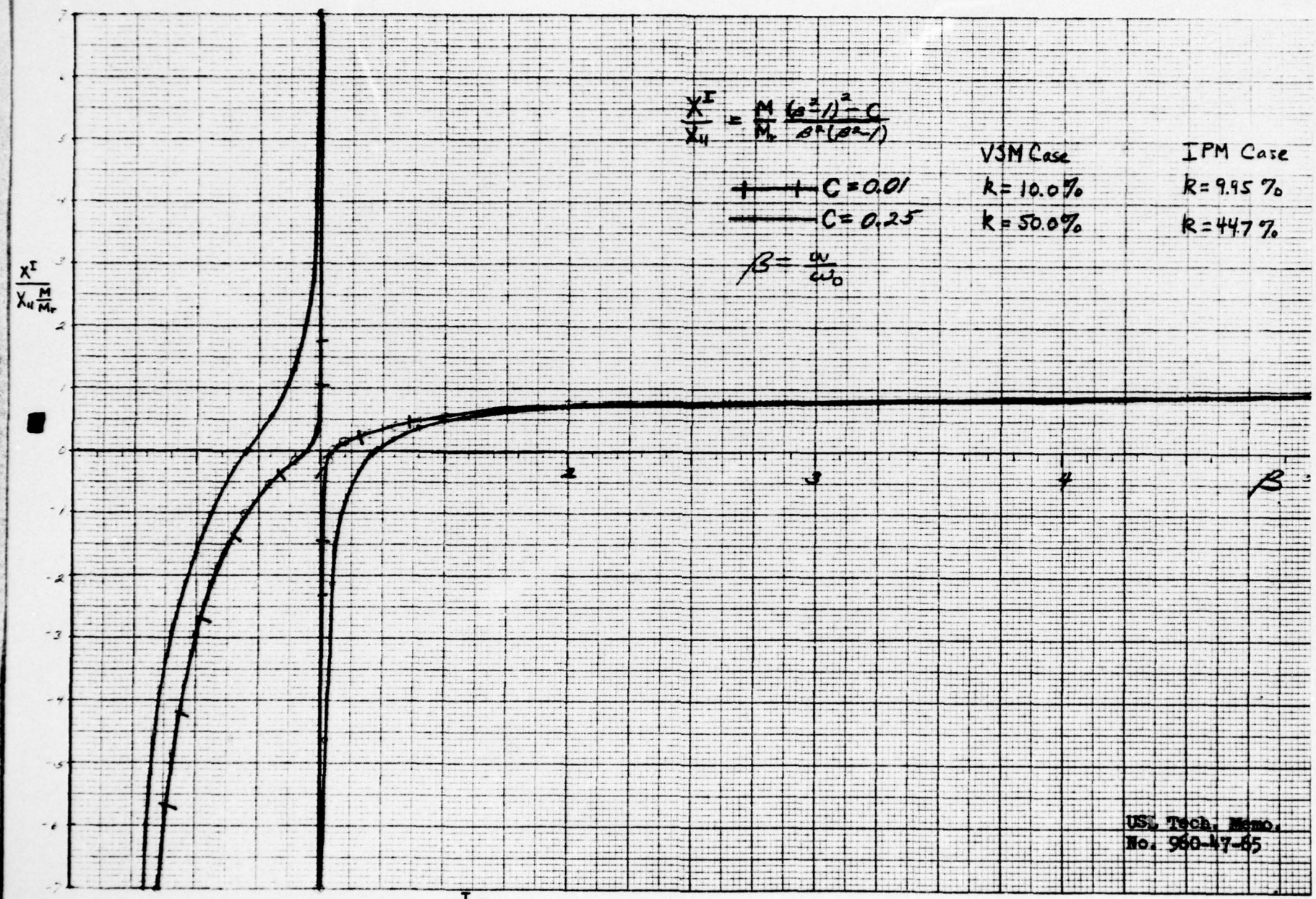

Figure 4d X^I/X_{11} for VSM, IPM Cases

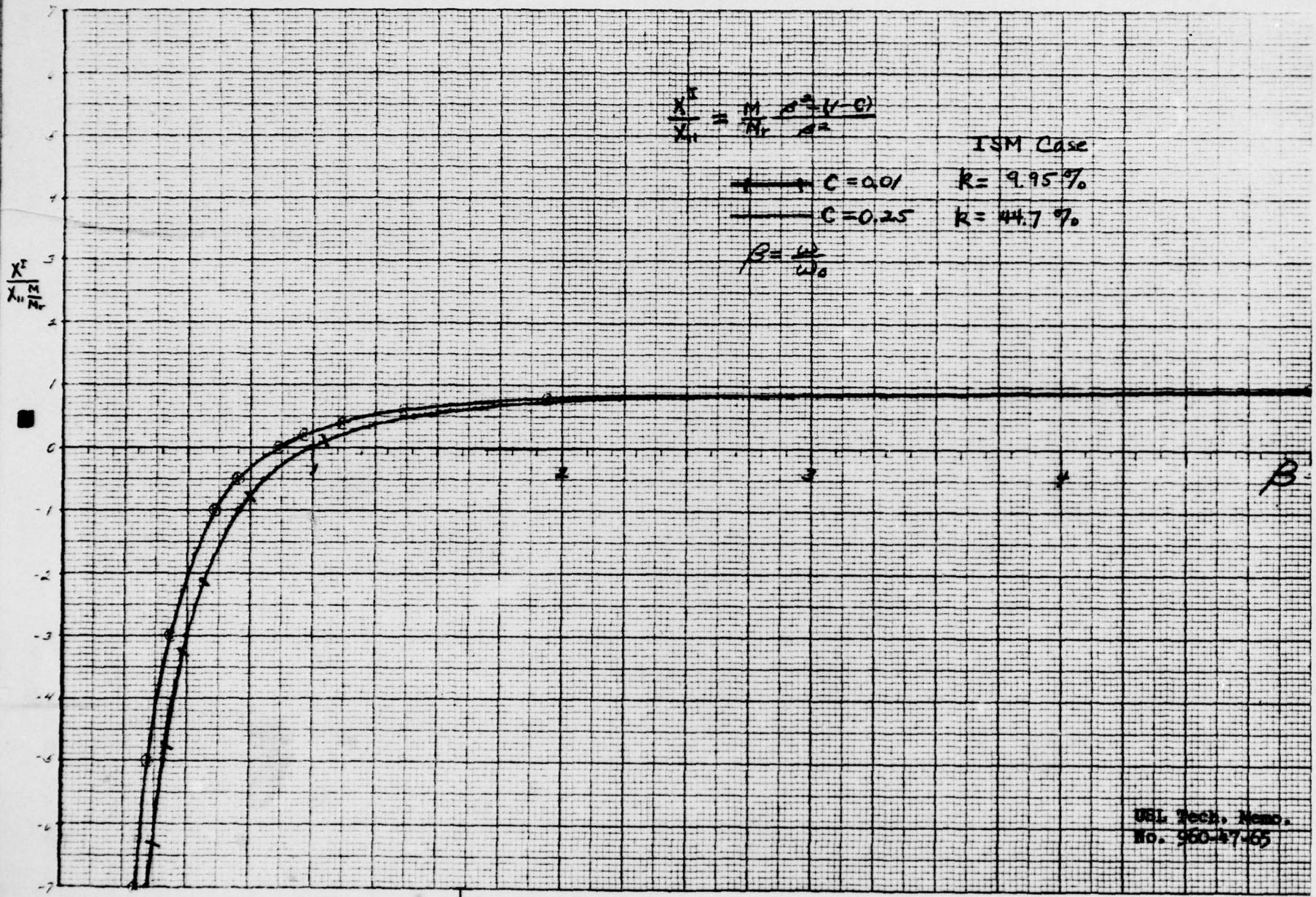

Figure 4e X^I/X_{11} for ISM Case